

# Investigation Nonlinear Properties (First and Second Hyperpolarizabilities) of The Nitro-thieno [3,2-b] thiophene -fullerene (C<sub>20</sub>) Molecule

Samira Resan\*, Mhanned Al-Anber

Department of Physics, College of Science, University of Basrah, Basrah, Iraq.

\*Corresponding Author.

Received 26/02/2023, Revised 19/05/2023, Accepted 21/05/2023, Published Online First 20/11/2023



This work is licensed under a [Creative Commons Attribution 4.0 International License](https://creativecommons.org/licenses/by/4.0/).

## Abstract

In this study, nonlinear optical (NLO) properties of nitro-thieno [3,2-b] thiophene-fullerene (C<sub>20</sub>) molecule was systematically investigated using density functional theory (DFT) methods at the B3LYP level with a 6-31 + G(d,p) basis set. Fullerene (electron-donor) is associated with thieno [3,2-b] thiophene ( $\pi$ -conjugated bridge), forming a charge-transfer framework, and nitro is a strong electron-acceptor. The dynamic properties of the molecule, including first and second hyperpolarizability, resulting from second harmonic generation  $\beta(-2\omega; \omega, \omega)$ , third harmonic generation  $\gamma(-2\omega; \omega, \omega, \omega)$ , Pockels effect  $\beta(-\omega; \omega, 0)$ , and Kerr effect  $\gamma(-\omega; \omega, 0, 0)$ , were investigated, which are essential evaluation indexes for creating nonlinear materials. The molecule exhibits excellent nonlinear responses, where it was found that the highest linear response of the coefficients above at the wavelength 455.6 nm. Absorption spectra reveal that these molecules have infrared transparent regions and are novel nonlinear molecules. Therefore, linking nitro-thieno[3,2-b]thiophene with fullerene (C<sub>20</sub>) efficiently designs high-performance nonlinear molecules.

**Keywords:** Density functional theory, Kerr effect, Pockels's effect, Second harmonic generation, Third harmonic generation.

## Introduction

A great deal of attention has long been paid to the nonlinear optical properties of organic compounds, mainly because of their importance in photonic, optoelectronic, and other devices that use light to carry information<sup>1</sup>. Optical switches, sensors, modulators, harmonic generators, optical computing, optical data processing, optical data storage, and optical limiting effects are all examples of applications for nonlinear materials<sup>2,3</sup>. Almost all NLO materials in the last 30 years were made of inorganic crystals<sup>4</sup>. Because organic materials have greater NLO responses than inorganic counterparts, there has recently been a paradigm shift toward them<sup>5-7</sup>. Moreover, they may be made cheaply, and they form high-quality crystals quickly.

Additionally, they can be easily integrated into thin films, they can be easily integrated into thin films since they have excellent solution processability. Therefore, they can be dissolved or dispersed in suitable solvents before being deposited on various substrates by methods such as spin coating or dip coating. They additionally have flexible molecular architectures, which indicate they can be modified or designed to achieve desired properties or functions in thin films<sup>8,9</sup>. Molecules containing electron donor (D) and electron acceptor (A) groups linked by the conjugated bridge are frequently used to create effective NLO materials<sup>7,10</sup>. The NLO activities of these push-pull molecules are due to intramolecular charge transfer between D and A group<sup>11</sup>. Organic

materials are the first class of materials to offer nonlinear optical features, and they are attractive candidates for synthesis because of their possible applicability in modern devices. It displays striking NLO behavior in the visual spectrum. Extensive research has shown that varying the donor/acceptor substituents, conjugation length, and dimensionality of the  $\pi$ -electron system can improve the NLO characteristics of organic materials. Although NLO materials research has advanced significantly, it has not yet attained the level necessary for practical applications<sup>12-14</sup>. To comprehend the connection between the structure and NLO properties of organic materials, theoretical calculations of molecular structure and third-order NLO characteristics are necessary<sup>3</sup>. Density functional theory (DFT) in particular has been extremely effective in this area, according to computational chemistry methods<sup>15</sup>. Therefore, this method was chosen since it is quicker than experimental and other theoretical methods and yields like results. To investigate the NLO properties of structures with stronger electron donor groups, DFT is used<sup>16,17</sup>. The NLO activities of the proposed molecules are enhanced when appropriate donor groups are used to promote intramolecular charge transfer (ICT)<sup>18</sup>. Excellent NLO responses are often seen in donor-acceptor (D-A) push-pull complexes caused by intramolecular charge transfer between donor(D) and acceptor(A)<sup>19</sup>. Electron donors and acceptors are groups of atoms that can donate or accept electrons, respectively. In NLO materials, electron donors and acceptors are often connected by a  $\pi$ -conjugated system, which is a chain of atoms with alternating single and double bonds that allow for the delocalization of  $\pi$ -electrons<sup>20</sup>. This forms a push-pull structure, where the electron donor pushes electrons to the  $\pi$ -system and the electron acceptor pulls electrons from the  $\pi$ -system. This creates an intramolecular charge transfer (ICT) process, which enhances the NLO response of the material. According to computational results, the first and second hyperpolarizabilities can be significantly enhanced. Thus, density functional theory may be reliable for calculating the electronic contributions to nonlinear optical properties for organic fullerenes<sup>21-23</sup> or nanotubes<sup>16</sup>.

In this work, nitro-thieno [3,2-b] thiophene - fullerene (NTTF) has been designed as an NLO

structure with five phases, as shown in Fig. 1. One of our goals is to analytically assess the NLO behavior of nitro-thieno [3,2-b] thiophene -fullerene at the first and second polarizability (NTTF) using the DFT quantum mechanical approach. In addition, DFT/B3LYP has defined HOMOs and LUMOs, as the highest and lowest occupied molecular orbitals respectively.

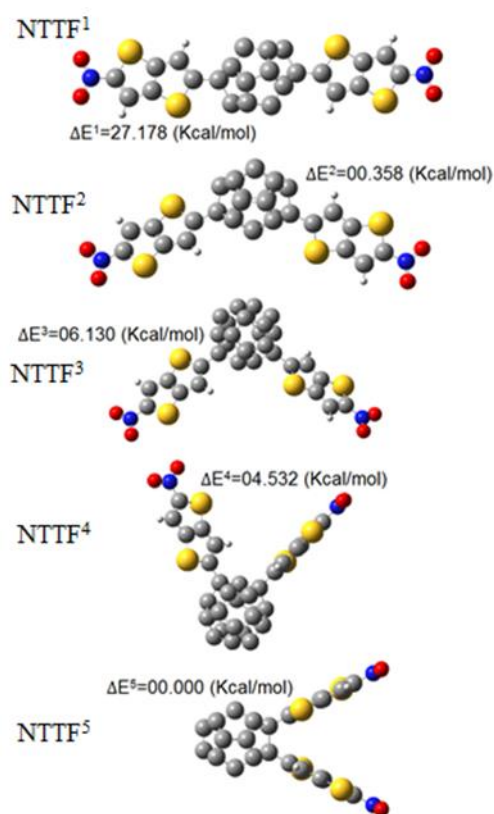


**Figure 1. The optimized geometry of the design NLO structure (nitro-thieno [3,2-b] thiophene-fullerene (C20)) of the five phases (NTTF<sup>1</sup>, NTTF<sup>2</sup>, NTTF<sup>3</sup>, NTTF<sup>4</sup> and NTTF<sup>5</sup> respectively) using the B3LYB/6-31+G(d,p) method.**

### Theoretical Calculations

The ground-state geometry optimizations for nitro-thieno [3,2-b] thiophene-fullerene (C20) five molecular phases, see Fig. 1, have been explored by performing DFT calculations, where all calculations are in the gas phase. The choice of a suitable computational method is crucial when calculating NLO properties. Using Gaussian 09 can conduct DFT (density functional theory) calculations based

on quantum mechanic<sup>24</sup>. The NLO properties were calculated using the DFT/B3LYP/6-311+G(d,p) method, which was chosen for its efficiency and precision. B3LYP functional combines Becke's three exchange parameters and Lee-Yang-Parr correlation parameters<sup>25</sup>. In a homogeneous electric field, the energy of a molecular system is expressed as follows<sup>26</sup>:

$$E = E_0 - \mu_i F_i - \frac{1}{2!} \alpha_{ij} F_i F_j - \frac{1}{3!} \beta_{ijk} F_i F_j F_k - \frac{1}{4!} \gamma_{ijkl} F_i F_j F_k F_l - \dots \quad 1$$

where  $E_0$  is the total energy of the molecule lacking the presence of an electric field,  $F_i$  is the applied electric field in the  $i$  direction, and  $\mu_i$ ,  $\alpha_{ij}$ ,  $\beta_{ijk}$ , and  $\gamma_{ijkl}$  are the molecular permanent dipole moment, polarizability, and first and second hyperpolarizability tensors, respectively. The total dipole moments ( $\mu$ ), average polarizabilities ( $\alpha_0$ ), anisotropy polarizabilities ( $\Delta\alpha$ ), first hyperpolarizabilities ( $\beta$ ), and second hyperpolarizabilities ( $\gamma$ ) are expressed as follows<sup>26</sup>:

$$\mu = (\mu_x^2 + \mu_y^2 + \mu_z^2)^{\frac{1}{2}} \quad 2$$

## Results and Discussion

This work shows the results of the theoretical design of NLO molecules. In the case of A- $\pi$ -D- $\pi$ -A systems NLO properties were considered because they have the characteristic and ability of intramolecular charge transfer between D and A through the  $\pi$ -bridge. For this investigation, it was essential to determine the most stable form of NLO design structure (nitrothieno [3,2-b] thiophene -fullerene (C20)) that has five phases (NTTF<sup>1</sup>, NTTF<sup>2</sup>, NTTF<sup>3</sup>, NTTF<sup>4</sup> and NTTF<sup>5</sup>), see Fig 1. Where according to the relative energy  $\Delta E$ , two phases, NTTF<sup>5</sup> and NTTF<sup>3</sup>, are favored over the three others. Polarization is a measure of how the electric dipole moment of a molecule changes in response to an applied electric field. Polarization can be divided into linear polarization and nonlinear polarization, depending on whether the electric field is weak or strong. Linear

$$\alpha_0 = \frac{1}{3} (\alpha_{xx} + \alpha_{yy} + \alpha_{zz}) \quad 3$$

$$\Delta\alpha = 2^{-1/2} \left[ (\alpha_{xx} - \alpha_{yy})^2 + (\alpha_{yy} - \alpha_{zz})^2 + (\alpha_{zz} - \alpha_{xx})^2 + 6\alpha_{xz}^2 + 6\alpha_{xy}^2 + 6\alpha_{yz}^2 \right]^{1/2} \quad 4$$

$$\beta_{tot} = (\beta_x^2 + \beta_y^2 + \beta_z^2)^{\frac{1}{2}} \quad 5$$

where  $\beta$  is the third rank tensor and is expressed as a  $3 \times 3 \times 3$  matrix. Conferring to Kleinman symmetry ( $\beta_{xyy} = \beta_{yyx} = \beta_{yyx} = \beta_{yyz} = \beta_{zyy} = \beta_{zyy}, \dots$  likewise and these 27 components can be reduced to 10 (Kleinman 1962)<sup>27</sup> and Gaussian 09 output provides ten components of this matrix as  $\beta_{xxx}$ ;  $\beta_{xxy}$ ;  $\beta_{xyy}$ ;  $\beta_{yyy}$ ;  $\beta_{xxz}$ ;  $\beta_{xyz}$ ;  $\beta_{yyz}$ ;  $\beta_{xzz}$ ;  $\beta_{yzz}$ ;  $\beta_{zzz}$ , respectively<sup>28</sup>, in atomic units (AU), so that  $\beta_x = (\beta_{xxx} + \beta_{xyy} + \beta_{xzz})$ ,  $\beta_y = (\beta_{yyy} + \beta_{yzz} + \beta_{yxx})$ ,  $\beta_z = (\beta_{zzz} + \beta_{zxx} + \beta_{zyy})$ <sup>29</sup>.

The optical dispersion in the medium has been ignored in the present work, so it is possible to calculate the average (or absolute value) of static second hyperpolarizability by applying Kleinman's 43 formula<sup>30</sup>:

$$\gamma = \frac{1}{5} (\gamma_{xxxx} + \gamma_{yyyy} + \gamma_{zzzz} + 2\gamma_{xxyy} + 2\gamma_{xxzz} + 2\gamma_{yyzz}) \quad 6$$

polarization is proportional to the electric field, while nonlinear polarization is proportional to higher powers of the electric field<sup>31</sup>. And, anisotropy of polarizability is a measure of how the polarizability of a molecule varies with different directions of the electric field. Anisotropy of polarizability can affect the NLO properties of a molecule, such as its second harmonic generation (SHG) and two-photon absorption (TPA) coefficients<sup>32</sup>. The modification of molecular structure, such as donor-acceptor configuration, usually increases polarization, but this effect is more pronounced for anisotropy of polarizability  $\Delta\alpha(-\omega; \omega)$  at the low wavelengths. This is because the donor-acceptor configuration induces a large ICT transition dipole moment that is perpendicular to the  $\pi$ -conjugated system, which creates a large difference between the parallel and

perpendicular components of polarizability. This difference increases as the wavelength decreases, because the ICT transition becomes more dominant compared to other transitions<sup>32</sup>. Therefore, donor-acceptor configuration can enhance the NLO response of a molecule by increasing its anisotropy of polarizability at the low wavelengths.

To comprehend dynamic NLO properties like polarizability  $\alpha_o(-\omega, \omega)$ , the first response of a molecule to an applied external electric field, it is necessary to calculate the response of tensor components of dynamic hyperpolarizabilities on a molecular level. The isotropy and anisotropy polarizability is represented as  $\alpha_o(-\omega; \omega)$  and  $\Delta\alpha(-\omega; \omega)$ , respectively. Where the dynamic polarizability

$\alpha_o(-\omega; \omega)$  and  $\Delta\alpha(-\omega; \omega)$  values, are showing in Fig 2, increase as the input frequency increases. It is observed that the calculated results of the average linear polarizability  $\alpha_o(-\omega; \omega)$  have values that are not negligible, but the wavelength 455.6 nm had the highest value, according to the following order NTTF<sup>3</sup>, NTTF<sup>4</sup>, and NTTF<sup>1</sup>, NTTF<sup>2</sup>. Anisotropic polarizability  $\Delta\alpha(-\omega; \omega)$  was ordered as NTTF<sup>5</sup>, NTTF<sup>1</sup>, NTTF<sup>3</sup>, NTTF<sup>2</sup>, and NTTF<sup>4</sup>, see Fig.2. Hence, the polarizability results are higher at  $\lambda = 455.6$  nm and decreases as the frequency decrease. The modification of molecular structure, such as donor-acceptor configuration, usually increases polarization, but this effect is more pronounced for anisotropy of polarizability  $\Delta\alpha(-\omega; \omega)$  at the low wavelengths, as given in Fig 2.

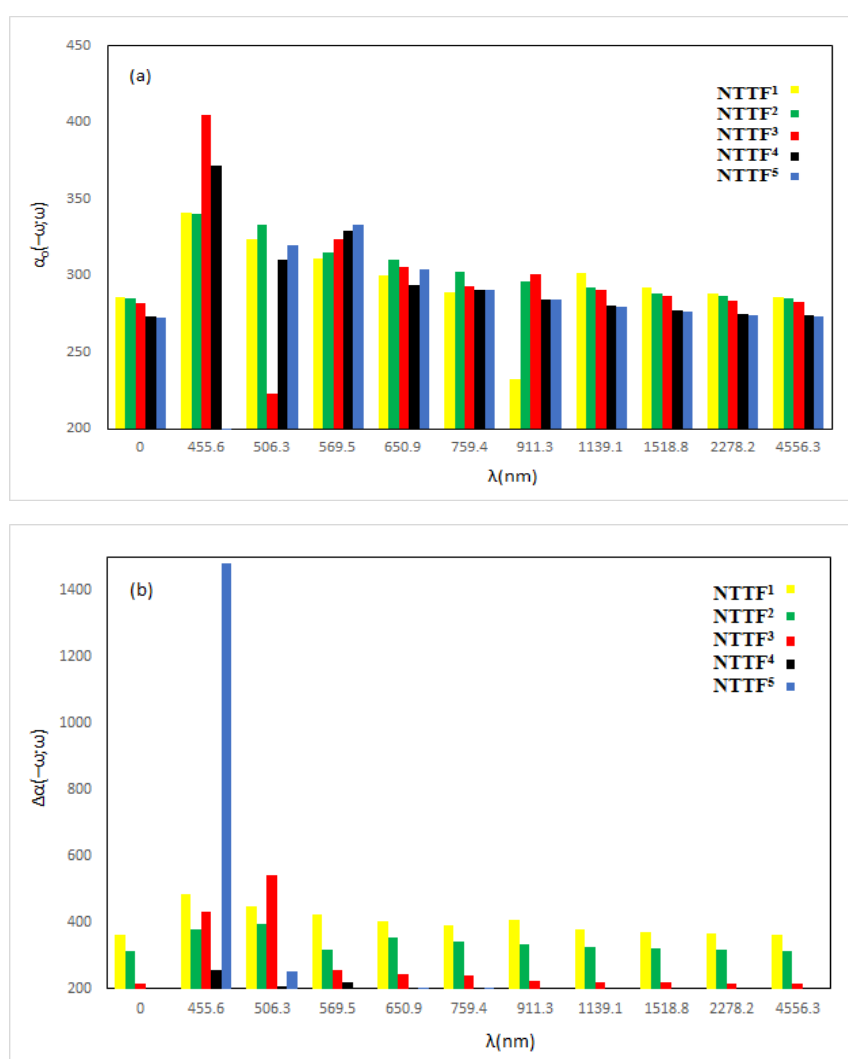


**Figure 2. a) The isotropy  $\alpha_o(-\omega, \omega)$  and b) anisotropy polarizability  $\Delta\alpha(-\omega, \omega)$  of NTTF<sup>1</sup>, NTTF<sup>2</sup>, NTTF<sup>3</sup>, NTTF<sup>4</sup> and NTTF<sup>5</sup> with respective values of wavelengths.**

Frequency-dependent simulations have been conducted to understand the title molecule's nonlinearity. The first hyperpolarizability  $\beta(\omega)$  included assessing Pockel's effect  $\beta(-\omega;\omega,0)$  and second harmonic generation  $\beta(-2\omega;\omega,\omega)$ , Whereas the second hyperpolarizability included Kerr effect  $\gamma(-\omega;\omega,0,0)$ , second harmonic generation (SHG)  $\gamma(-2\omega;\omega,\omega,0)$  and third harmonic generation (THG)  $\gamma(-3\omega;\omega,\omega,\omega)$ . The range of frequencies from 455.6 to 4556.3 nm was chosen to validate dynamic nonlinearity.

Pockels effect, which is a change in the refractive index in proportion to the electric field of light. It depends on the material and the light wavelength. Pockel's effect  $\beta(-\omega; \omega,0)$  at 455.6 nm, see Fig 3, are ordered as NTTF<sup>5</sup>, NTTF<sup>3</sup>, NTTF<sup>2</sup>, NTTF<sup>1</sup>, and

NTTF<sup>4</sup>, where the NTTF<sup>5</sup> showed an 50% increase compared with NTTF<sup>3</sup>. Pockel's effect is the linear electro-optic effect, where the refractive index of a medium is modified in proportion to the applied electric field strength, where the refractive index depends on Pockel's coefficient, this means the refractive index increases with Pockel's effect. Based on the computed values, Pockel's influence is similarly stronger at lower wavelengths.

Second harmonic generation  $\beta(-2\omega;\omega,\omega)$  showed that at a frequency of 455.6 nm, the order is NTTF<sup>5</sup>, NTTF<sup>3</sup>, NTTF<sup>4</sup>, NTTF<sup>2</sup>, and NTTF<sup>1</sup>, see Fig 4. There was a 250% increase in NTTF<sup>5</sup> compared to NTTF<sup>3</sup>. At 506.3 nm  $\beta(-2\omega;\omega,\omega)$  they are ordered as NTTF<sup>2</sup>, NTTF<sup>3</sup>, NTTF<sup>5</sup>, and NTTF<sup>4</sup>.

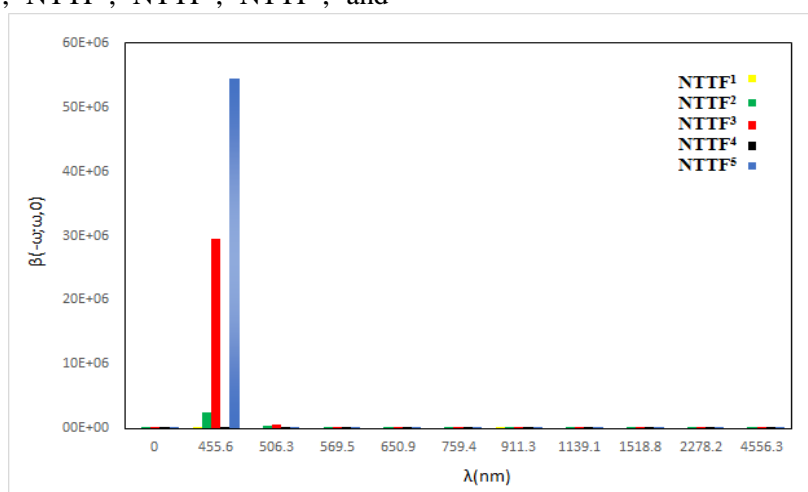


**Figure 3.** Pockel's effect  $\beta(-\omega;\omega,0)$  of NTTF<sup>1</sup>, NTTF<sup>2</sup>, NTTF<sup>3</sup>, NTTF<sup>4</sup> and NTTF<sup>5</sup> with respective values of wavelengths.

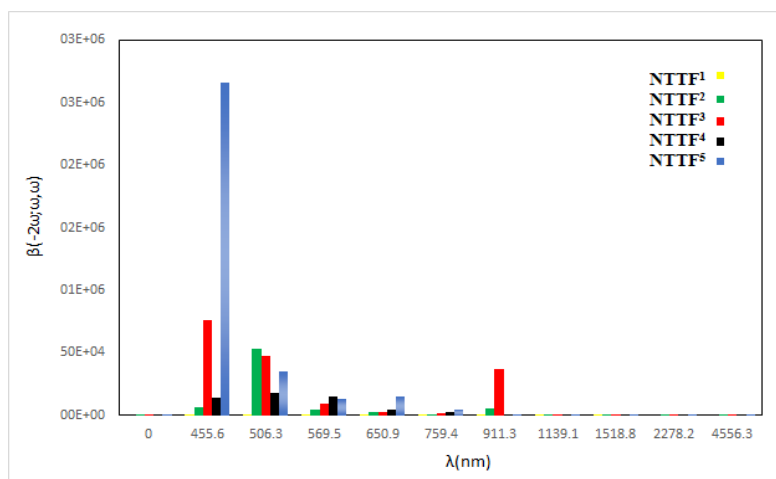


**Figure 4.** Second harmonic generation  $\beta(-2\omega;\omega,\omega)$  of NTTF<sup>1</sup>, NTTF<sup>2</sup>, NTTF<sup>3</sup>, NTTF<sup>4</sup> and NTTF<sup>5</sup> with respective values of wavelengths.

The second hyperpolarizability (THG) is calculated by the Kerr effect  $\gamma(\omega;\omega,0,0)$  and second harmonic generation  $\gamma(2\omega;\omega,\omega,0)$  and the third harmonic generation hyperpolarizability  $\gamma(-3\omega;\omega,\omega,\omega)$  for the title molecules.

Kerr effect of the molecule, which is a change in the refractive index of a material in response to an applied electric field<sup>33</sup>. The refractive index measures how light when it passes through a material. The Kerr effect is different from the Pockels effect in that the change in refractive index is proportional to the square of the electric field instead of varying linearly with it<sup>33</sup>. The Kerr effect

values are increased, which means that the change in refractive index is large for a given electric field. This also implies that the molecule has a large Kerr constant, which determines how much the refractive index changes. Kerr effect  $\gamma(-\omega; \omega,0,0)$  values at 455.6 nm are ordered as NTTF<sup>4</sup>, NTTF<sup>5</sup>, and NTTF<sup>3</sup>, respectively, see Fig 5. At 455.6 nm, the greatest computed Kerr effect  $\gamma(-\omega; \omega,0,0)$  increased by 500% for NTTF<sup>4</sup> compared to NTTF<sup>5</sup>. At the same time, the remaining phases are almost vanishing. The greater Kerr effect values also show that the examined molecule's refractive index changes nonlinearly.

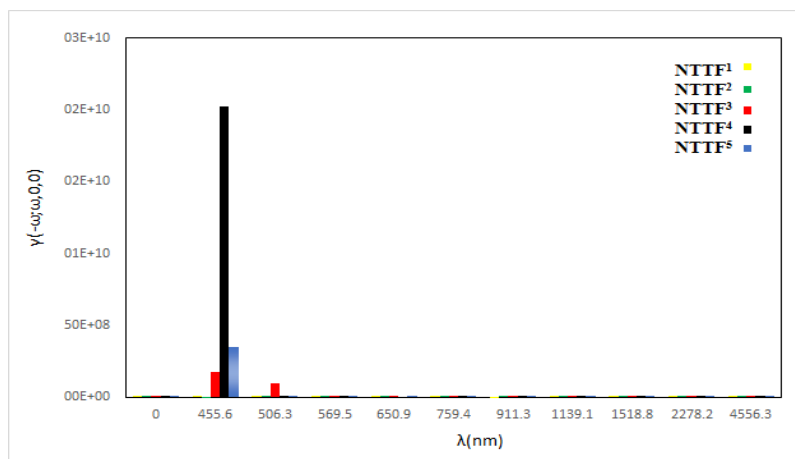


**Figure 5. Kerr effect values for NTTF<sup>1</sup>, NTTF<sup>2</sup>, NTTF<sup>3</sup>, NTTF<sup>4</sup> and NTTF<sup>5</sup> with respective values of wavelengths.**

As for the case of the second hyperpolarizability  $\gamma(-2\omega;\omega,\omega,0)$  is different, where all phases have high values at 455.6 nm in the order of NTTF<sup>3</sup>, NTTF<sup>5</sup>,

NTTF<sup>4</sup>, and NTTF<sup>2</sup>, as shown in Fig 6. While at 569.5 nm, NTTF<sup>5</sup> is significant. Finally, NTTF<sup>2</sup> has a very large value of 4556.3.

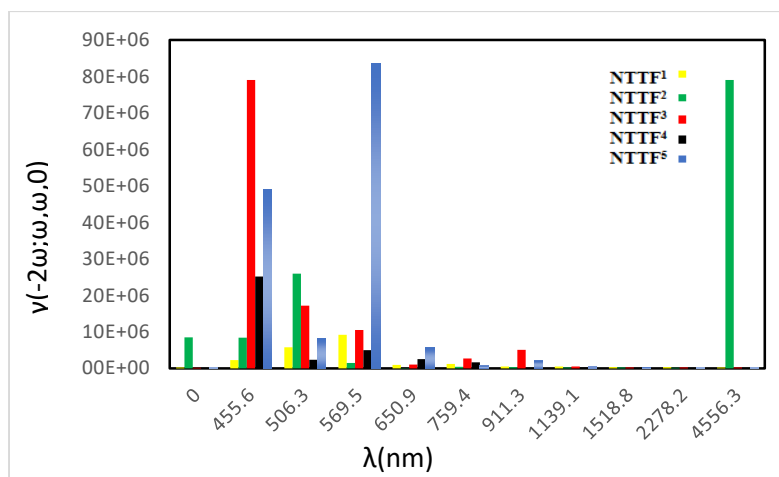


**Figure 6. Second hyperpolarizability  $\gamma(-2\omega;\omega,\omega,0)$  of NTTF<sup>1</sup>, NTTF<sup>2</sup>, NTTF<sup>3</sup>, NTTF<sup>4</sup> and NTTF<sup>5</sup> with respective values of wavelengths.**

Third harmonic generation  $\gamma(-3\omega; \omega, \omega, \omega)$  behaves quite similarly to the Kerr effect  $\gamma(-\omega; \omega, 0, 0)$ , where the NTTF<sup>4</sup> shows the highest value at 455.6 nm, and they are ordered as NTTF<sup>4</sup>, NTTF<sup>5</sup>, and NTTF<sup>3</sup>, see Fig 7. The interaction of the hyperpolarizability components within the molecule is seen to enhance with an increase in the electric field frequency, leading to greater values of the NLO coefficients. In

second hyperpolarization materials, Kerr nonlinearity produces self-phase and cross-phase modulation, two nonlinear effects. From the foregoing, it can be concluded that the dynamic second hyperpolarizability response of NTTF<sup>4</sup> to different optical frequencies is helpful for adjusting its second-order NLO effects in various applications.

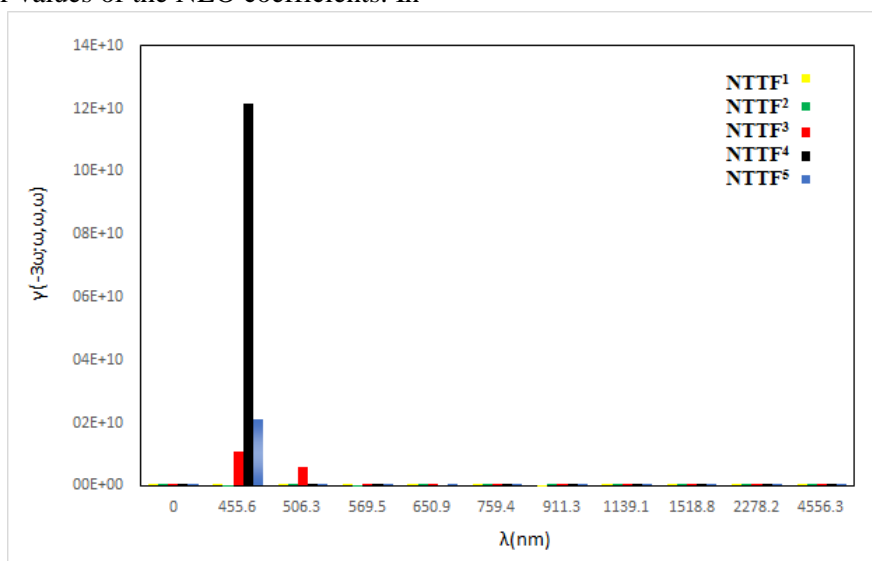


**Figure 7. Third harmonic generation hyperpolarizability  $\gamma(-3\omega; \omega, \omega, \omega)$  of NTTF<sup>1</sup>, NTTF<sup>2</sup>, NTTF<sup>3</sup>, NTTF<sup>4</sup> and NTTF<sup>5</sup> with respective values of wavelengths.**

## Conclusion

NLO properties of NTTF were studied using the DFT quantum method. The molecules' electronic absorption spectra were also analyzed using the TD-DFT approach (B3LYP), and the basis set 6-31+G(d,p). Before conducting NLO studies, the most stable conformer of NTTF was determined through conformational analysis. In this study, the dynamic NLO properties have been examined, including second harmonic generation (SHG), Pockels effect, third harmonic generation (THG) and Kerr effect. Charge delocalization and hyperpolarizability of NTTF are likely to be attributed to the conjugated

structures of thieno [3,2-b] thiophene in the NTTF molecule, where it was found that the highest linear response of the coefficients above at the wavelength 455.6 nm, it can be concluded that as electron acceptor capacity increases and the strength of the donor, dynamic hyperpolarizability increases. Due to its appealing nonlinear optical properties, the NTTF molecule is an excellent contender for creating novel photonic and optoelectronic devices, especially for third-order nonlinear applications, according to the second hyperpolarizability data.

## Authors' Declaration

- Conflicts of Interest: None.
- We hereby confirm that all the Figures and Tables in the manuscript are ours. Furthermore, any Figures and images, that are not ours, have been

- included with the necessary permission for republication, which is attached to the manuscript.
- Ethical Clearance: The project was approved by the local ethical committee in University of Basrah.

## Authors' Contribution Statement

S. R. and M. Al. conceived and designed the study. Calculations, data collection and analysis, were performed by S. R. . The second author (M. Al.) wrote the initial draft of the manuscript, and S. R.

commented and added some discussions on the initial version. Both authors read and approved the final manuscript.

## References

1. Mohbiya DR, Sekar N. Electronic structure and spectral properties of indole based fluorescent styryl dyes: Comprehensive study on linear and non-linear optical properties by DFT/TDDFT method. *Comput Theor Chem.* 2018; 1139(April): 90–101. <https://dx.doi.org/10.1016/j.comptc>.
2. Kiven DE, Nkungli NK, Tasheh SN, Ghogomu JN. In silico screening of ethyl 4-[(E)-(2-hydroxy-4-methoxyphenyl) methyleneamino] benzoate and some of its derivatives for their NLO activities using DFT. *R Soc Open Sci.* 2023; 10(1): 220430. <https://dx.doi.org/10.1098/rsos.220430>
3. Bibi A, Muhammad S, UrRehman S, Bibi S, Bashir S, Ayub K, et al. Chemically Modified Quinoidal Oligothiophenes for Enhanced Linear and Third-Order Nonlinear Optical Properties. *ACS Omega.* 2021; 6(38): 24602–24613. <https://dx.doi.org/10.1021/acsomega.1c03218>
4. Chen X, Ok KM. Metal oxyhalides: an emerging family of nonlinear optical materials. *Chem Sci.* 2022;13(14): 3942–3956. <https://dx.doi.org/10.1039/D1SC07121A>
5. Li Q, Li Z. Molecular packing: another key point for the performance of organic and polymeric optoelectronic materials. *Acc Chem Res.* ACS Publications; 2020; 53(4): 962–973. <https://dx.doi.org/10.1021/acs.accounts.0c00060>
6. Wang H-Y, Ye J-T, Qiu Y-Q, Chen F. Toward the design of inorganic–organic hybrid Ir(III) complexes containing borazine and benzene ligands with excellent second-order NLO responses: An appropriate substitution and  $\pi$ -conjugated extension. *J Mol Liq.* 2022; 612: 121081. <https://dx.doi.org/10.1016/j.molliq.2022.121081>
7. Rasool F, Hussain A, Yar M, Ayub K, Sajid M, Ali M, et al. Nonlinear optical response of 9,10-bis(phenylethynyl)anthracene mediated by electron donating and electron withdrawing substituents: A density functional theory approach. *Mat Sci Semicond Process.* 2022;148(May): 106751. <https://dx.doi.org/10.1016/j.mssp>.
8. Sulka GD. Electrochemistry of Thin Films and Nanostructured Materials. *Molecules.* 2023; 28(10), 4040. <https://dx.doi.org/10.3390/molecules28104040>
9. Butt A. Thin-Film Coating Methods: A Successful Marriage of High-Quality and Cost-Effectiveness—A Brief Exploration. *Coatings.* 2022; 12(8), 1115. <https://dx.doi.org/10.3390/coatings12081115>
10. Derkowska-Zielinska B, Barwiolek M, Cassagne C, Boudebs G. Nonlinear optical study of Schiff bases using Z-scan technique. *J Opt Laser Technol.* 2020; 124: 105968. <https://dx.doi.org/10.1016/j.optlastec.2019.105968>
11. Pant D, Darla N, Sitha S. Roles of various bridges on intramolecular charge Transfers, dipole moments and first hyperpolarizabilities of Donor-Bridge-Acceptor types of organic Chromophores: Theoretical assessment using Two-State model. *Comput. Theor. Chem.* 2022;1209: 113583. <https://dx.doi.org/10.1016/j.comptc.2021.113583>
12. Li H-PP, Bi Z-TT, Xu R-FF, Han K, Li M-XX, Shen X-PP, et al. Theoretical study on electronic polarizability and second hyperpolarizability of hexagonal graphene quantum dots: Effects of size, substituent, and frequency. *Carbon.* 2017;122: 756–760. <https://dx.doi.org/10.1016/j.carbon.2017.07.033>
13. Singh P, Kumar A, Reena, Gupta A, Patil PS, Prabhu S, et al. Vibrational spectroscopic characterization, electronic absorption, optical nonlinearity computation and terahertz investigation of (2E) 3-(4-ethoxyphenyl)-1-(3-bromophenyl) prop-2-en-1-one for NLO device fabrication. *J Mol Struct.* 2019; 1198: 126909. <https://dx.doi.org/10.1016/j.molstruc.2019.126909>
14. Bahrani F, Hameed R, Resan S, M Al-anber M. Impact of Torsion Angles to Tune Efficient Dye-Sensitized Solar Cell/Donor- $\pi$ -Acceptor Model Containing Triphenylamine: DFT/TD-DFT Study. *Acta Phys Pol A.* 2022; 141(6): 561–568. <https://dx.doi.org/10.12693/APhysPolA.141.561>
15. Bulik IW, Zaleśny R, Bartkowiak W, Luis JM, Kirtman B, Scuseria GE, et al. Performance of density functional theory in computing nonresonant vibrational (hyper) polarizabilities. *J Comput Chem.* 2013; 34(20): 1775–1784. <https://dx.doi.org/10.1002/jcc.23316>
16. Resan S, Hameed R, Al-Hilo A, Al-Anber M. The impact of torsional angles to tune the nonlinear optical response of chalcone molecule: Quantum



- computational study. *Rev Cub Fis.* 2020; 37(2): 95–100.  
<http://www.revistacubanadefisica.org/index.php/rcf/article/view/2020v37p095>.
17. Kubba RM, Mohammed MA, Ahamed LS. DFT calculations and experimental study to inhibit carbon steel corrosion in saline solution by quinoline-2-one derivative. *Baghdad Sci J.* 2021; 18(1): 113–123.  
<https://dx.doi.org/10.21123/bsj.2021.18.1.0113>
18. Samanta PK, Misra R. Intramolecular charge transfer for optical applications. *Appl. Phys.* 2023;133(2).  
<https://dx.doi.org/10.1063/5.0131426>
19. Ahn M, Kim MJ, Cho DW, Wee KR. Electron Push-Pull Effects on Intramolecular Charge Transfer in Perylene-Based Donor-Acceptor Compounds. *J. Org. Chem.* 2021;86(1): 403–413. <https://dx.doi.org/10.1021/acs.joc.0c02149>
20. Huang Y, Zhou W, Li X, Jiang L, Song Y. Highly broadband NLO response of acceptor-donor-acceptor materials with a planar conformation. *Mat Adv.* 2021; 2(6): 2097–2103.  
<https://dx.doi.org/10.1039/d0ma00918k>
21. Shinde SS, Sreenath MC, Chitrambalam S, Joe IH, Sekar N. Spectroscopic, DFT and Z-scan approach to study linear and nonlinear optical properties of Disperse Red 277. *Opt Mater.* 2020; 99(August): 109536.  
<https://dx.doi.org/10.1016/j.optmat.2019.109536>
22. Al-Anber MJ, Al-Mowali AH, Ali AM. Theoretical semiempirical study of the nitron (anticancer drug) interaction with fullerene C60 (as delivery). *Acta Phys Pol A.* 2014; 126(3): 845–848.  
<https://dx.doi.org/10.12693/APhysPolA.126.845>
23. Al-anber MJ. Theoretical Semi-empirical Study of the Glycine Molecule Interaction with Fullerene C60. *Electron J Chem.* 2014; 6(3): 156–160.  
<http://www.orbital.ufms.br/index.php/Chemistry/article/view/491>
24. Frisch M J, Trucks Gary, Schlegel H B, Scuseria G E, Robb Michael A, Cheeseman James R, et al. 'Gaussian 09, Revision A. 02. Gaussian Inc, Wallingford, CT.' See also: URL: <http://www.gaussian.com.2009;2009>.
25. Halls MD, Velkovski J, Schlegel HB. Harmonic frequency scaling factors for Hartree-Fock, S-VWN, B-LYP, B3-LYP, B3-PW91 and MP2 with the Sadlej pVTZ electric property basis set. *Theor Chem Acc.* 2001; 105(6): 413–421.  
<https://dx.doi.org/10.1007/s002140000204>
26. Mathew E, Salian V V., Hubert Joe I, Narayana B, Joe IH, Narayana B. Third-order nonlinear optical studies of two novel chalcone derivatives using Z-scan technique and DFT method. *J Opt Laser Technol.* 2019; 120: 105697.  
<https://dx.doi.org/10.1016/j.optlastec.2019.105697>
27. Khalid M, Hussain R, Hussain A, Ali B, Jaleel F, Imran M, et al. Electron donor and acceptor influence on the nonlinear optical response of diacetylene-functionalized organic materials (DFOMs): Density functional theory calculations. *Molecules.* 2019;24(11).  
<https://dx.doi.org/10.3390/molecules24112096>
28. Kubba RM, Kadhim MM. Reactivity of O-Drug Bond in some Suggested Voltarine Carriers: Semiempirical and ab Initio Methods. *Baghdad Sci J.* 2021; 18(4): 1249. <https://dx.doi.org/10.21123/bsj.2021.18.4.1249>
29. Günay N, Tamer Ö, Avci D, Tarcan E, Atalay Y. Molecular modelling, spectroscopic characterization and nonlinear optical analysis on N-Acetyl-DL-methionine. *Rev Mex de Fis.* 2020; 66(6): 749–760.  
<https://dx.doi.org/10.31349/revmexfis.66.749>
30. Begam S, Deepa M, Ummal M, Hu J, Guin M. Effect of fluorination on bandgap, first and second order hyperpolarizabilities in lithium substituted adamantane: A time dependent density functional theory. *Chem Phys Lett.* 2019; 715: 310–316.  
<https://dx.doi.org/10.1016/j.cplett.2018.11.034>
31. Gorman CB, Marder SR. Effect of Molecular Polarization on Bond-Length Alternation, Linear Polarizability, First and Second Hyperpolarizability in Donor-Acceptor Polyenes as a Function of Chain Length. *Chem Mater.* 1995; 7(1): 215–220.  
<https://dx.doi.org/10.1021/cm00049a033>.
32. Li S, He M, Jin X, Geng W, Li C, Li X, et al. Extending the Stokes Shifts of Donor–Acceptor Fluorophores by Regulating the Donor Configuration for In Vivo Three-Photon Fluorescence Imaging. *Chem Mater.* 2022; 34(13): 5999–6008.  
<https://dx.doi.org/10.1021/acs.chemmater.2c01025>
33. Mbarak H, Kodeary AK, Hamidi SM, Mohajarani E, Zaatar Y. Control of nonlinear refractive index of AuNPs doped with nematic liquid crystal under external electric field. *Optik.* 2019; 198: 163299.  
<https://dx.doi.org/10.1016/j.ijleo.2019.163299>

## دراسة الخصائص غير الخطية (قابلية الاستقطاب المفرط الأول والثاني) لجزيء نيترو ثينو [2،3-ب] ثيوفين-فوليرين (C20)

سميرة فاخر رسن، مهند جاسم العنبر

قسم الفيزياء، كلية العلوم، جامعة البصرة، البصرة، العراق.

### الخلاصة

في هذه الدراسة، تم فحص الخصائص البصرية غير الخطية (NLO) لجزيء نيترو-ثينو [2،3-ب] ثيوفين-فوليرين (C20) بشكل منهجي باستخدام طرق نظرية الكثافة الوظيفية (DFT) على مستوى B3LYP مع مجموعة الأساس 6-31+G(d,p). يرتبط الفوليرين (المتبرع بالإلكترون) مع ثينو [2،3-ب] ثيوفين ( $\pi$ -جسر مترافق)، مما يشكل إطارًا لنقل الشحنة، والنيترو هو متقبل قوي للإلكترون. تمت دراسة الخصائص الديناميكية للجزيء، بما في ذلك فرط الاستقطاب الأول والثاني، مما أدى إلى التوليد التوافقي الثاني  $\beta(-2\omega; \omega, \omega)$  والتوليد التوافقي الثالث  $\gamma(-2\omega; \omega, \omega, \omega)$  وتأثير Pockels  $\beta(-\omega; \omega, 0)$  وتأثير Kerr  $\gamma(-\omega; \omega, 0, 0)$ ، هي فهارس تقييم مهمة لإنشاء مواد لاخطية. يُظهر الجزيء استجابات لاخطية ممتازة، وهي فهارس تقييم مهمة لإنشاء مواد لاخطية. حيث وجد أن أعلى استجابة خطية للمعاملات أعلاه عند الطول الموجي 455.6 نانومتر. تكشف أطيف الامتصاص أن هذه الجزيئات لها مناطق شفافة تحت الحمراء وجزيئات لاخطية جديدة. لذلك، فإن ربط [3-nitro-thieno] 2-b ثيوفين بالفوليرين (C20) هو طريقة فعالة لتصميم جزيئات لاخطية عالية الأداء.

**الكلمات المفتاحية:** نظرية الكثافة الوظيفية، تأثير كبير، تأثير بوكل، التوليد التوافقي الثاني، التوليد التوافقي الثالث.